

# Developmental Dynamics

Volume 239 • Number 1 • January 2010

SPECIAL ISSUE ON WNT IN DEVELOPMENT AND DISEASE



Gary C. Schoenwolf  
Editor-in-Chief

# The Trimeric G Protein Go Inflicts a Double Impact on Axin in the Wnt/Frizzled Signaling Pathway

Diane Egger-Adam and Vladimir L. Katanaev\*

The Wnt/Frizzled signaling pathway plays crucial roles in animal development and is deregulated in many cases of carcinogenesis. We and others have previously demonstrated that Frizzled proteins initiating the intracellular signaling are typical G protein-coupled receptors and rely on the trimeric G protein Go for Wnt transduction in *Drosophila*. However, the mode of action of Go and its interplay with other transducers of the pathway such as Dishevelled and Axin remained unclear. Here we show that the  $\alpha$ -subunit of Go directly acts on Axin, the multidomain protein playing a negative role in the Wnt signaling. G $\alpha$  physically binds Axin and re-localizes it to the plasma membrane. Furthermore, G $\alpha$  suppresses Axin's inhibitory action on the Wnt pathway in *Drosophila* wing development. The interaction of G $\alpha$  with Axin critically depends on the RGS domain of the latter. Additionally, we show that the  $\beta\gamma$ -component of Go can directly bind and recruit Dishevelled from cytoplasm to the plasma membrane, where activated Dishevelled can act on the DIX domain of Axin. Thus, the two components of the trimeric Go protein mediate a double—direct and indirect—impact on different regions of Axin, which likely serves to ensure a robust inhibition of this protein and transduction of the Wnt signal. *Developmental Dynamics* 239:168–183, 2010. © 2009 Wiley-Liss, Inc.

**Key words:** Wnt; Frizzled; G proteins; Axin; Dishevelled; *Drosophila*

Accepted 6 July 2009

## INTRODUCTION

The Wnt signaling pathway is highly conserved in animal evolution and controls multiple developmental programs during organism development (Logan and Nusse, 2004). This pathway is also important for adult physiology and pathology, being involved in stem cell proliferation (Reya and Clevers, 2005), brain function (De Ferrari and Moon, 2006), and carcinogenesis (Polakis, 2007) among other things. Wnt signaling is initiated by secreted glycoproteins of the Wnt family, which consists of 19 members in humans and

7 in *Drosophila*. On the cell surface, two types of proteins serve as co-receptors for the Wnt ligands. The first is a single-pass transmembrane protein of the low-density lipoprotein receptor protein type (LRP5 or LRP6 in vertebrates, Arrow in flies; He et al., 2004). The second is a G protein-coupled receptor of the Frizzled (Fz) family, which includes 10 members in humans and 4 in *Drosophila* (Wang et al., 2006).

On the cytoplasmic side, a crucial function in Wnt signaling is played by the so-called destruction complex.

This complex is built by the scaffolding protein Axin (of which there are two isoforms in mammals and one in flies), which, through its multiple domains, binds the adenomatous polyposis coli (APC) protein, glycogen synthase kinase 3 (GSK3), casein kinase 1 (CK1), and  $\beta$ -catenin (Luo and Lin, 2004; Kimelman and Xu, 2006). The consequence of this binding is a set of phosphorylations on  $\beta$ -catenin, which target this protein for ubiquitin-dependent proteosomal degradation (Aberle et al., 1997).

When the Wnt ligand activates its

Additional Supporting Information may be found in the online version of this article.  
Department of Biology, University of Konstanz, Konstanz, Germany

Grant sponsor: Deutsche Forschungsgemeinschaft; Grant number: TransRegio-SFB11.

\*Correspondence to: Vladimir L. Katanaev, Universitätsstrasse 10, Box 643, D-78457 Konstanz, Germany.

E-mail: vladimir.katanaev@uni-konstanz.de

DOI 10.1002/dvdy.22060

Published online 21 August 2009 in Wiley InterScience (www.interscience.wiley.com).

co-receptors LRP5/6 and Fz, a series of biochemical reactions leads to recruitment of Axin to the plasma membrane and dissociation of the destruction complex (Mao et al., 2001; Cliffe et al., 2003; Tolwinski et al., 2003). Cytoplasmic  $\beta$ -catenin is no longer phosphorylated or degraded, enters the nucleus, and with the help of multiple cofactors activates transcription of the target genes, which are characterized by the specific enhancer regions binding Lymphoid enhancer factor/T cell factor proteins (LEF/TCF, pangolin in flies) (Willert and Jones, 2006).

Axin re-localization to the plasma membrane in response to Wnt pathway activation is thought to proceed through at least two routes. First, Axin can be directly bound by the cytoplasmic tail of LRP5/6 (Mao et al., 2001), which can be further enhanced by its phosphorylation by CK1 and GSK3 (Tamai et al., 2004; Davidson et al., 2005; Zeng et al., 2005). This interaction depends on the DIX and the central domains of Axin (Mao et al., 2001). Second, the multidomain protein Dishevelled (Dsh) interacts with several components of the  $\beta$ -catenin destruction complex including Axin (Malbon and Wang, 2006). This binding occurs through heterodimerization of the DIX domains present in both Dsh and Axin (Cliffe et al., 2003; Schwarz-Romond et al., 2007).

Dsh by itself is a cytoplasmic protein that is recruited to the plasma membrane upon activation of the Wnt pathway. The main mechanism of Dsh re-localization is believed to be the direct binding of Dsh to the C-terminus of Fz receptors demonstrated for the mammalian proteins (Wong et al., 2003; Punchihewa et al., 2009). However, some of the tested Fz-Dsh pairs interacted only with a low micromolar affinity, while others completely failed in the physical interaction, despite their physiological cooperation (Wong et al., 2003; Punchihewa et al., 2009). Another mechanism has been recently proposed to involve a polybasic stretch of amino acids in the DEP domain of *Drosophila* Dsh, which can directly bind the phospholipids of the plasma membrane (Simons et al., 2009). However, it is unclear how this interaction can be regulated during signaling. Furthermore, it is not necessary for the Wnt-Fz pathway (Simons et al.,

2009). Thus, other ways of Dsh plasma membrane recruitment during Fz activation are likely to exist.

Fz receptors belong to the G protein-coupled receptor superfamily (Fredriksson et al., 2003), which utilizes trimeric G proteins as their immediate cytoplasmic binding partners and transducers (Gilman, 1987). Trimeric G proteins consist of the  $\alpha$ -,  $\beta$ -, and  $\gamma$ -subunits. In the resting trimeric state of the G protein, the  $\alpha$ -subunit is bound to GDP. Upon ligand binding, the G protein-coupled receptor adopts an activated conformation and acts as a guanine nucleotide exchange factor towards the trimeric G protein, catalyzing the substitution of GDP for GTP on the  $\alpha$ -subunit. This exchange leads to dissociation of the trimeric complex into G $\alpha$ -GTP and the  $\beta\gamma$ -heterodimer. Both can engage downstream signal transduction effectors (Milligan and Kostenis, 2006).

Fz receptor signaling in many contexts depends on trimeric G proteins in insects and vertebrates (Malbon, 2005; Egger-Adam and Katanaev, 2008). Malbon and co-workers have demonstrated that stimulation of rat Fz-1 in F9 mouse teratocarcinoma cells induced  $\beta$ -catenin-dependent responses through trimeric G proteins Go and Gq (Liu et al., 1999, 2001; Feigin and Malbon, 2007). Experiments in *Drosophila* revealed an important function of Go in the Wnt/Fz pathway (Katanaev et al., 2005); no other trimeric G protein has so far been implicated in *Drosophila* Wnt signaling (Egger-Adam and Katanaev, 2008). We demonstrated with genetic (Katanaev et al., 2005; Katanaev and Tomlinson, 2006) and biochemical studies (Katanaev and Buestorf, 2009) that Fzs, as typical G protein-coupled receptors, directly activate trimeric G proteins. Using epistasis experiments, Go was shown to act downstream from Fz receptors but upstream from Dsh in the Wnt pathway (Katanaev et al., 2005; Feigin and Malbon, 2007). Additionally, biochemical experiments in the L929 and 3T3-L1 cells revealed that within minutes of cell stimulation with Wnt3a, trimeric G proteins mediated the dissociation of the GSK3-Axin protein complexes (Liu et al., 2005). Interestingly, Gq acted on the GSK3-Axin complexes and Go acted on the GSK3-Axin2 complexes

(Liu et al., 2005). Since Axin possesses an RGS domain known in other proteins to bind G $\alpha$ -subunits of trimeric G proteins (Dohlman and Thorner, 1997; Castellone et al., 2005; Stemmler et al., 2006), these experiments hint at the possibility that this scaffolding protein might be another target of trimeric G proteins in the Wnt pathway.

In the present article, we demonstrate that *Drosophila* Axin is indeed a direct interaction partner of G $\alpha$ -GTP in the Wnt signal transduction and that this interaction occurs through the RGS domain of Axin. We also show evidence suggesting that the  $\beta\gamma$ -component of the trimeric Go protein acts to recruit and activate Dsh, which in turn also acts on Axin. This double impact of the trimeric Go protein on Axin serves to efficiently disorganize the Axin-based  $\beta$ -catenin destruction complex and propagate the Wnt signal within the cell.

## RESULTS

### Activated G $\alpha$ Re-Localizes *Drosophila* Axin to the Plasma Membrane

Axin becomes rapidly re-localized to the plasma membrane upon signal activation (Fagotto et al., 1999; Cliffe et al., 2003; Schwarz-Romond et al., 2007; Yokoyama et al., 2007). G $\alpha$  is required for Wnt signaling and can over-activate the Wnt signal transduction upon over-expression (Katanaev et al., 2005). The GTP-loaded form of G $\alpha$  is the active species of this G protein in Wnt signaling; expression of the wild-type form of G $\alpha$  activates signaling only in the presence of active Fz receptors, which act as guanine nucleotide exchange factors and charge G $\alpha$  with GTP (Katanaev et al., 2005; Katanaev and Tomlinson, 2006; Katanaev and Buestorf, 2009). Due to post-translational lipid modifications such as myristoylation (Wedegaertner et al., 1995), a large part of G $\alpha$  is constantly bound to the plasma membrane (Fig. 1A–C).

To test whether G $\alpha$  might directly induce plasma membrane localization of Axin, we expressed the wild-type or the constitutively GTP-loaded forms of G $\alpha$  (Katanaev et al., 2005) along with Axin-GFP in the giant salivary gland cells of *Drosophila* larvae. This



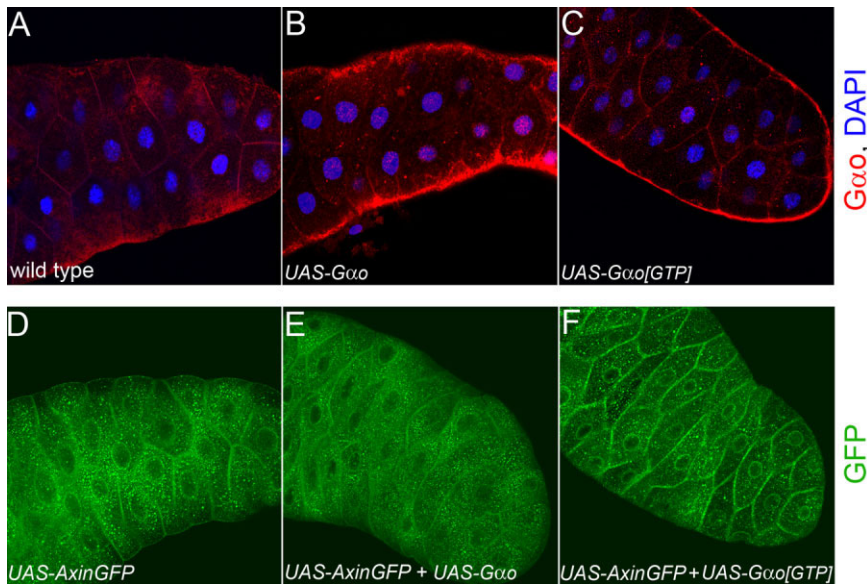


**Fig. 1.** Activated  $G\alpha o$  is able to relocate Axin to the plasma membrane in salivary glands. Endogenous  $G\alpha o$  (A), as well as over-expressed  $G\alpha o$  (B) and  $G\alpha o[GTP]$  (C), all show mostly plasma membrane-associated staining (red; nuclei stained in blue). Axin-GFP (green) expressed in salivary glands is localized in the cytoplasm, at the perinuclear membrane, and in part at the plasma membrane (D). Over-expression of  $G\alpha o[GTP]$  (F), but not  $G\alpha o$  (E), re-localizes Axin-GFP to the plasma membrane.

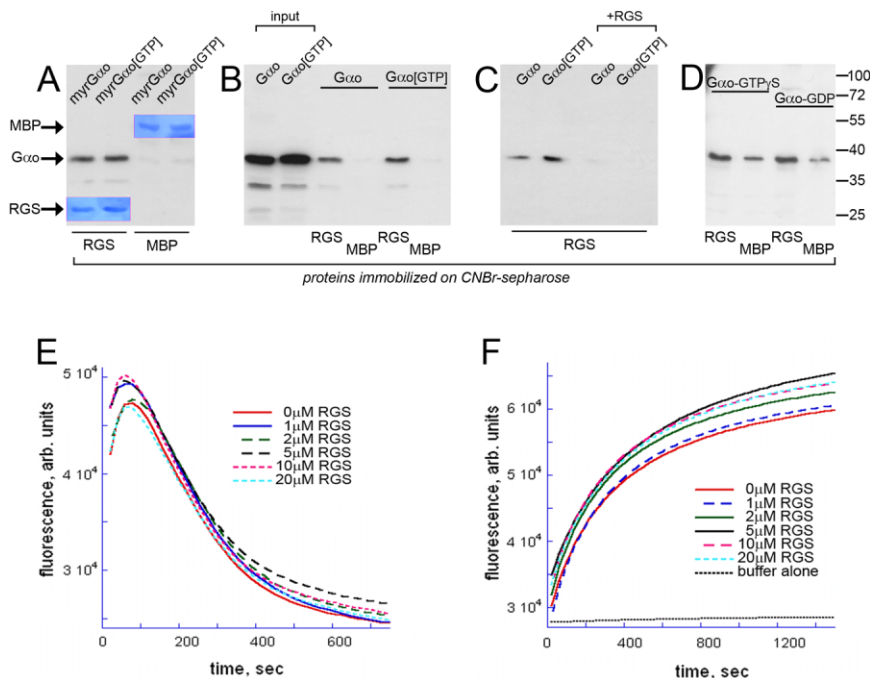


**Fig. 2.** The RGS domain of Axin can directly interact with but does not change activity of  $G\alpha o$ . **A:** Pull-down with the RGS domain of Axin immobilized on a matrix (RGS) but not with the control matrix (MBP) precipitates equally the recombinant myristoylated  $G\alpha o$  and  $G\alpha o[GTP]$  proteins, as detected by anti- $G\alpha o$  Western blot. The blue inserts are Coomassie staining of the membrane showing that equal amounts of RGS and MBP were used. **B:** A similar pull-down assay using non-modified  $G\alpha o$  and  $G\alpha o[GTP]$ . **C:** A competition experiment with soluble RGS protein ("RGS") is shown. **D:** Purified  $G\alpha o$  preloaded with either GTPγS or GDP also binds to RGS. **E,F:** The kinetics of GTP hydrolysis (E) or binding (F) by  $G\alpha o$  is not influenced by increasing concentrations of the RGS domain of Axin.

Axin-GFP construct is fully functional in the Wnt pathway (Cliffe et al., 2003); its expression in wing imaginal discs causes the expected and strong down-regulation of the Wnt target genes (data not shown, also see below). Figure 1D shows that Axin-GFP alone localizes mostly in the cytoplasm with low plasma membrane and perinuclear membrane staining. Co-expression of  $G\alpha o$  does not significantly affect this localization pattern (Fig. 1E). In contrast, expression of  $G\alpha o[GTP]$  induces a massive and almost complete re-localization of Axin-GFP to the plasma membrane (Fig. 1F). The extent of Axin re-localization induced by  $G\alpha o[GTP]$  in salivary glands (Fig. 1F) is similar to that observed in other cells upon activation of the Wnt pathway (Cliffe et al., 2003; Schwarz-Romond et al., 2007). Thus, generation of high levels of  $G\alpha o[GTP]$  is sufficient to mimic the activation of Fz and LRP5/6 receptors by the Wnt ligands. These experiments reveal a possibility that Axin is a direct target of  $G\alpha o[GTP]$  in the Wnt signal transduction.

### $G\alpha o$ Physically Binds the RGS Domain of Axin

Axin possesses an N-terminal RGS domain that is known in other proteins to bind directly the GTP-loaded forms of  $G\alpha$ -subunits of trimeric G proteins (Dohlman and Thorner, 1997). Furthermore, the RGS domain of mammalian Axin has been shown to interact with  $G\alpha s$  and  $G\alpha 12$  (Castellone et al., 2005; Stemmler et al., 2006). Thus, if a direct binding between *Drosophila* Axin and  $G\alpha o$  exists, it is likely to be mediated by the RGS domain.

To test this possibility, we generated RGS domain of Axin as a recombinant hexahistidine-tagged protein. After affinity purification from bacteria, His<sub>6</sub>-RGS was immobilized on CNBr-sepharose. A non-related protein (maltose-binding protein, MBP) was similarly immobilized as a control. Additionally, the following forms of recombinant  $G\alpha o$  were expressed in bacteria: (1) His<sub>6</sub>-tagged versions of  $G\alpha o$  and  $G\alpha o[GTP]$ ; (2) non-tagged forms of  $G\alpha o$  and  $G\alpha o[GTP]$ ; (3) non-tagged myristoylated forms of  $G\alpha o$  and  $G\alpha o[GTP]$ . These various forms of  $G\alpha o$  were applied to the Axin's RGS or

control matrixes and their ability to bind specifically to RGS was tested.

Figure 2A, B shows that G $\alpha$ , either its wild-type (and thus predominantly GDP-bound) or activated (and thus predominantly GTP-bound) form, provided in bacterial lysates, can equally bind the RGS domain of Axin. In contrast, the control matrixes (MBP-charged or empty) did not precipitate G $\alpha$  (Fig. 2A, B). The equal interaction of the GDP- and GTP-bound G $\alpha$  with Axin's RGS domain was seen with both myristoylated and the non-myristoylated forms of G $\alpha$  (Fig. 2A, B). The specificity of these interactions was further confirmed in a competition experiment, where addition of the soluble Axin's RGS to G $\alpha$  prevented the binding of the latter to the matrix-immobilized RGS (Fig. 2C). We also found the interaction of Axin's RGS with the purified His<sub>6</sub>-tagged G $\alpha$  directly charged with either GDP or GTP $\gamma$ S nucleotides (Fig. 2D), although significant amounts of G $\alpha$  also bound to the control matrixes in these experiments, probably due to the absence of bacterial proteins masking the unspecific G $\alpha$ -matrix interaction sites. Cumulatively, these data demonstrate for the first time the physical interaction between the RGS domain of *Drosophila* Axin and the G $\alpha$ -subunit of the trimeric Go protein.

### The RGS Domain of Axin Does Not Affect the GTP Binding and Hydrolysis Properties of G $\alpha$

Typically, the RGS proteins bind the GTP-loaded forms of G $\alpha$ -subunits to speed up the GTP hydrolysis reaction on the G $\alpha$  reviewed in Dohlman and Thorner, 1997). The fact that the Axin RGS domain does not differentiate between the GDP- and the GTP-forms of G $\alpha$  suggests that the nature of this interaction differs from the typical RGS-G $\alpha$  interactions. Indeed, the RGS domain of Axin lacks some of the conserved amino acids required for the GAP activity (Zeng et al., 1997; Sidarovski et al., 1999; Stemmler et al., 2006). To directly test whether the RGS domain of Axin could stimulate the GTPase reaction on G $\alpha$ , we performed the BODIPY-GTP hydrolysis reactions (Jameson et al., 2005) on G $\alpha$  in the presence of increasing concentrations of

Axin RGS. Up to a 20-fold excess of Axin RGS was unable to influence the GTPase reaction on G $\alpha$  (Fig. 2E). In contrast, the usage of a conventional RGS protein (*Drosophila* homolog of RGS19) in the same assay revealed a strong stimulation of the GTPase reaction (Lin and Katanaev, unpublished observations). Similarly, Axin RGS was unable to change the kinetics of GTP incorporation into G $\alpha$  (Fig. 2F), as measured by the BODIPY-GTP $\gamma$ S assay (McEwen et al., 2001). As a control, identical application of the GoLoco domains of Pins to G $\alpha$  was efficient in slowing down the GTP loading reaction (Kopein and Katanaev, 2009). Thus, our biochemical experiments demonstrate that the RGS domain of Axin is unable to affect the GTP loading or hydrolysis reactions on G $\alpha$ , in accordance with previous experiments on mammalian Axin and G $\alpha$  proteins (Castellone et al., 2005). We conclude that the physical interaction between Axin and G $\alpha$  described in the previous section does not change the kinetic properties of G $\alpha$ , but is likely to influence the activity of Axin in Wnt signaling. To test this possibility, we performed in vivo experiments, where we first investigated the importance of the RGS domain of Axin for its activity.

### The RGS Domain of Axin Is Important for Its Function

Contradictory data exist as to the importance of the RGS domain of Axin for its activity in the Wnt signaling. In vertebrates, this domain was found necessary for the full range of Axin activity (Zeng et al., 1997; Fagotto et al., 1999), and an Axin $\Delta$ RGS mouse knock-in construct was found to produce phenotypes identical to Axin loss-of-function (Chia et al., 2009). In contrast, over-expression of the Axin $\Delta$ RGS construct in *Drosophila* embryos produced inhibition of the Wnt pathway identical to that induced by the full-length Axin construct, which led to a proposition that the RGS domain of Axin was dispensable in *Drosophila* (Willert et al., 1999).

To investigate similarly the possible importance of the RGS domain in Axin function during wing development, we over-expressed the full-length or the  $\Delta$ RGS Axin constructs in the wing imaginal discs, and followed expression of the Wnt target genes. Two target

genes were analyzed: a long-range target gene Distal-less (Dll), which is normally expressed in the whole wing pouch, and a short-range target gene Senseless (Sens) expressed by the two stripes of cells immediately abutting the source of Wnt production (Fig. 3A). Expression of UAS-Axin $\Delta$ RGS and UAS-Axin full-length under the control of the *omb-Gal4* driver resulted in dramatic differences between the two constructs in their inhibition of the Wnt target gene expression (Fig. 3B, C). The full-length Axin construct produced a complete loss of expression of both targets in the region of over-expression (Fig. 3B). Furthermore, full-length Axin also resulted in growth defects, as the size of the *omb-Gal4* expression domain was strongly narrowed as compared to its normal broadness (compare Fig. 3A and B). Defective growth is a frequent outcome of a reduction in the Wnt signaling in the developing *Drosophila* wing (Johnston and Gallant, 2002; Katanaev et al., 2008) and can thus be used as another read-out of the Wnt transduction.

In contrast, similar expression of Axin $\Delta$ RGS had no influence on the disc growth and shape. Furthermore, the Dll expression was completely normal; it was only the short-range target gene Sens whose expression was lost in the region of over-expression (Fig. 3C). Markedly different levels of the intracellular Wnt signal transduction are required for the induction of expression of the short-range target genes like Sens and the long-range target genes like Dll (Katanaev et al., 2008). The efficiency of Axin $\Delta$ RGS to prevent Sens expression but not affect Dll expression suggests that this construct of Axin could reduce, but not fully inhibit, Wnt signaling. In contrast, similar expression of Axin full-length completely abrogated Wnt signaling. These data reveal a crucial role of the RGS domain for the activity of Axin.

The dramatic difference in the influence of the two Axin constructs on wing development could be further seen at the level of the adult wings. Axin $\Delta$ RGS only induced loss of the wing margin structures in the region of expression, not affecting the overall wing development (Fig. 3F). In contrast, Axin full-length almost completely prevented wing formation; only two chunks of the adult wing



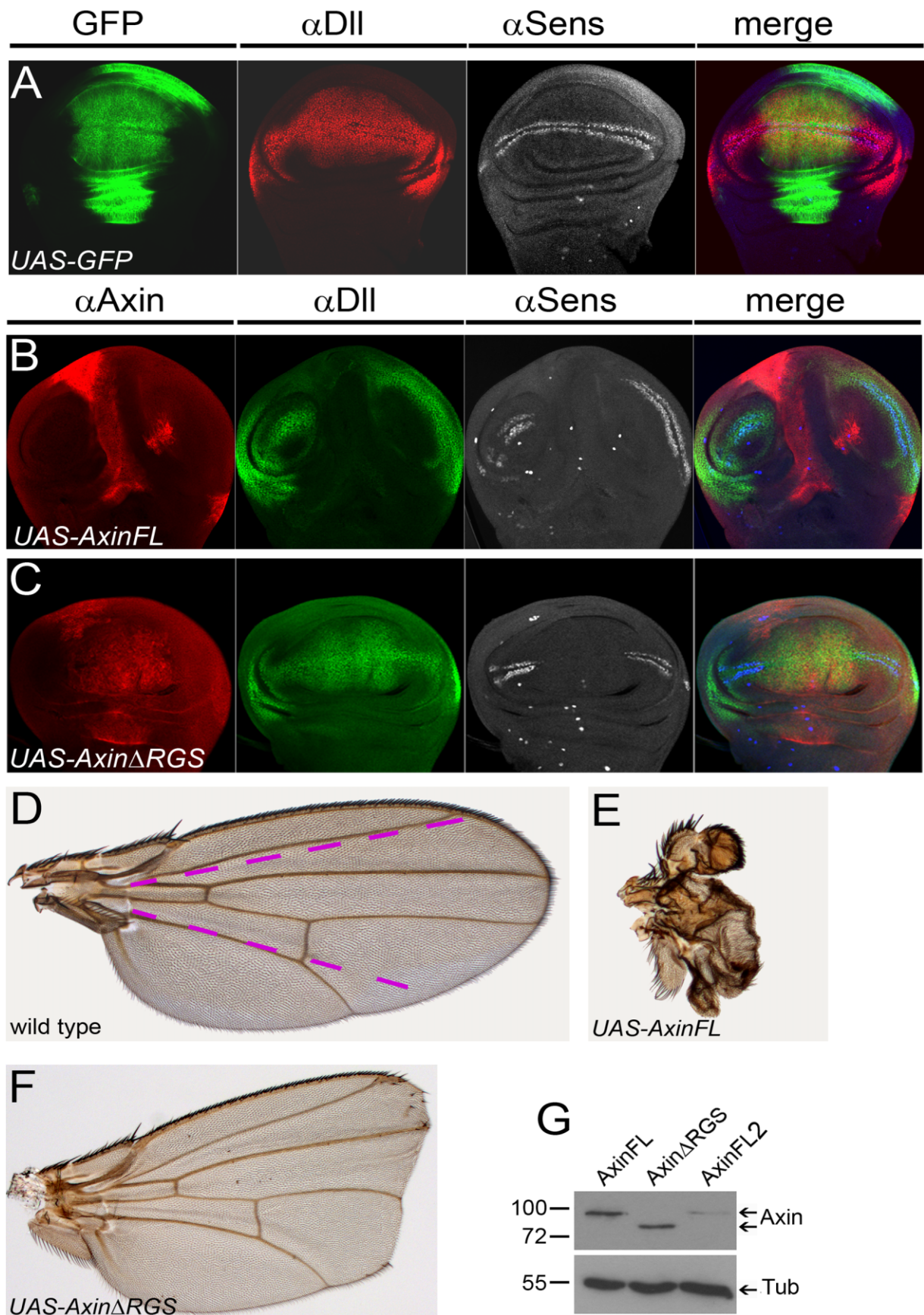


**Fig. 3.** The RGS domain plays an important role in Axin's activity in the Wnt pathway in wing imaginal discs. **A:** A disc expressing GFP (green) in the *omb-Gal4* region shows a wild-type staining for the Wnt target genes Dll (red) and Sens (grey). **B,C:** A similar expression of the full-length form of Axin (AxinFL, B) or Axin lacking the RGS domain (AxinΔRGS, C) leads to different effects on the broadness of the *omb-Gal4* zone (anti-Axin staining shown in red) and on Dll (green) and Sens (grey) expression. **D–F:** AxinFL and the AxinΔRGS constructs also induce different phenotypes in adult wings. The *omb-Gal4* expression zone is indicated between the two dashed pink lines on a wild-type wing (D). **G:** Equal expression levels are achieved with the AxinFL and AxinΔRGS constructs used for immunostainings above. Another full-length Axin construct (AxinFL2) gives lower expression levels.

structures remained corresponding to the regions where *omb-Gal4* was not active (Fig. 3E).

Expression levels of the two Axin constructs were similar. This can be seen at the level of the anti-Axin immunostaining in the wing discs (Fig. 3B, C). We additionally expressed the two constructs in salivary glands, isolated the glands, and performed the Western blot with anti-Axin antibodies to prove identical expression levels (Fig. 3G). We also obtained another independent UAS-Axin full-length construct, which resulted in lower levels of Axin over-expression (Fig. 3G). This construct produced weaker phenotypes when expressed in wing discs than the highly-expressing Axin full-length construct; however, these phenotypes were still more dramatic than those induced by the highly-expressing Axin $\Delta$ RGS construct and still completely abrogated both Sens and Dll expression (data not shown).

Overall, these data demonstrate a crucial role of the RGS domain of Axin for the full force of Axin activity in *Drosophila* wing development. As this domain can physically interact with G $\alpha$ , we next tested the physiologic consequences of this interaction.

### G $\alpha$ Partially Rescues the Axin Over-Expression Phenotypes

To investigate the potency of G $\alpha$  to interact with Axin in the physiologically relevant environment, we co-expressed Axin full-length with G $\alpha$  or G $\alpha$ [GTP] in wing imaginal discs. These forms of G $\alpha$  expressed in isolation induce an activation of the Wnt signaling in *Drosophila* wing discs (Katanaev et al., 2005). We found a remarkable, though incomplete, rescue of the Axin phenotypes by G $\alpha$ [GTP] (Fig. 4A, B). First, the morphology and growth properties of the wing discs were rescued upon G $\alpha$ [GTP] co-expression, as the *omb-Gal4* region became as broad as in the wild-type discs (compare the GFP-stained panel of Fig. 3A and the anti-Axin-stained panels of Fig. 4A, B). Second, a significant rescue of expression of both Dll and Sens within the Axin over-expression domain (constrained between the two dashed lines on Fig. 4B) could be seen.

The wild-type form of G $\alpha$  produced

a weaker, but still significant, rescue of the Axin phenotypes (Fig. 4C). A partial re-appearance of the Dll gene expression within the Axin over-expression zone (marked by the two dashed lines on Fig. 4C) could be seen. However, expression of Sens within the Axin zone was still absent (Fig. 4C). It should be noted that a general variability in Sens expression levels could be observed between discs; however, among >10 discs analyzed, no Sens expression could be seen inside the *omb-Gal4* region when Axin full-length was expressed alone or together with the wild-type G $\alpha$ . In contrast, in all discs co-expressing G $\alpha$ [GTP] a partial re-appearance of Sens within the Axin full-length-expressing domain was seen.

In wild-type G $\alpha$ -coexpressing discs, the size of the Axin expression domain was still reduced (Fig. 4C). At the same time, expression levels of the two G $\alpha$  constructs were approximately the same (Fig. 4B, C). These data indicate that the activated, GTP-loaded form of G $\alpha$  is most efficient in suppressing the phenotypes of Axin over-expression. However, no clear difference between the strength of the two G $\alpha$  forms was seen in the adult wings; both constructs produced a certain rescue of the Axin over-expression phenotypes (Fig. 4D–F), mostly seen as re-appearance of wing structures such as wing margins and veins (marked with brackets and arrowheads on Fig. 4D–F). However, these wings were still malformed. Additionally, many [Axin + G $\alpha$ [GTP]]-expressing flies died as late pupae due to unknown reasons and had to be extracted from the pupal cases for the wing analysis (which often resulted in mechanical breakage of the wings as on Fig. 4F). Thus, a more detailed comparison of the rescue efficiency of G $\alpha$  versus G $\alpha$ [GTP] was not possible at the level of the adult wings. A few flies in both genotypes showed a strong rescue of the wing shape and size (Fig. 4G).

### The Ability of G $\alpha$ to Rescue the Axin Over-Expression Phenotypes Critically Depends on the RGS Domain

Since G $\alpha$  binds physically to the RGS domain of Axin, we reasoned

that G $\alpha$  should be incapable of rescuing the Axin $\Delta$ RGS over-expression phenotypes. Indeed, adult wings co-expressing Axin $\Delta$ RGS and G $\alpha$ [GTP] showed no sign of improvement of the Axin $\Delta$ RGS phenotype (Fig. 5A, B). If anything, a certain worsening of the phenotype could be seen. Similarly, in wing imaginal discs no rescue of the Axin $\Delta$ RGS phenotypes could be obtained by co-expression of G $\alpha$ [GTP]; the size of the Axin $\Delta$ RGS expression domain, the lack of Sens expression, and the strength of Dll expression all remained the same between the two genotypes (Fig. 5D, E). These data clearly show that the capacity of G $\alpha$ [GTP] to suppress the activity of Axin critically depends on the presence of the RGS domain, as predicted from our biochemical experiments.

Paradoxically, the Axin $\Delta$ RGS phenotypes became much worse if the wild-type form of G $\alpha$  was co-expressed. Both at the level of the adult wing (Fig. 5C) and at the level of the wing imaginal disc (Fig. 5F), over-expression of G $\alpha$  forced the Axin $\Delta$ RGS phenotypes to approach or even fully reproduce those of over-expression of the full-length Axin (see Figs. 3 and 4). The morphology of the wing imaginal disc and the adult wing, the width of the region of expression of Axin/G $\alpha$ , and the expression pattern of Dll and Sens all revealed a strong enhancement of the phenotypes.

The unique enhancement of the Axin $\Delta$ RGS phenotypes by the wild-type form of G $\alpha$  is probably due to the fact that this form mostly resides in the GDP-bound state. To test this hypothesis, we co-expressed with Axin $\Delta$ RGS a mutant form of G $\alpha$  which is unable to bind GTP and thus resides always in the GDP-bound state (Katanaev et al., 2005). We find that this G $\alpha$ [GDP] protein worsens the Axin $\Delta$ RGS phenotypes similarly to G $\alpha$  (Fig. 5G). Overall, these experiments demonstrate a crucial role of the RGS domain of Axin in its physiological interaction with G $\alpha$ , as G $\alpha$ [GTP] fails to rescue, while G $\alpha$  and G $\alpha$ [GDP] even dramatically enhance the Axin $\Delta$ RGS phenotypes.



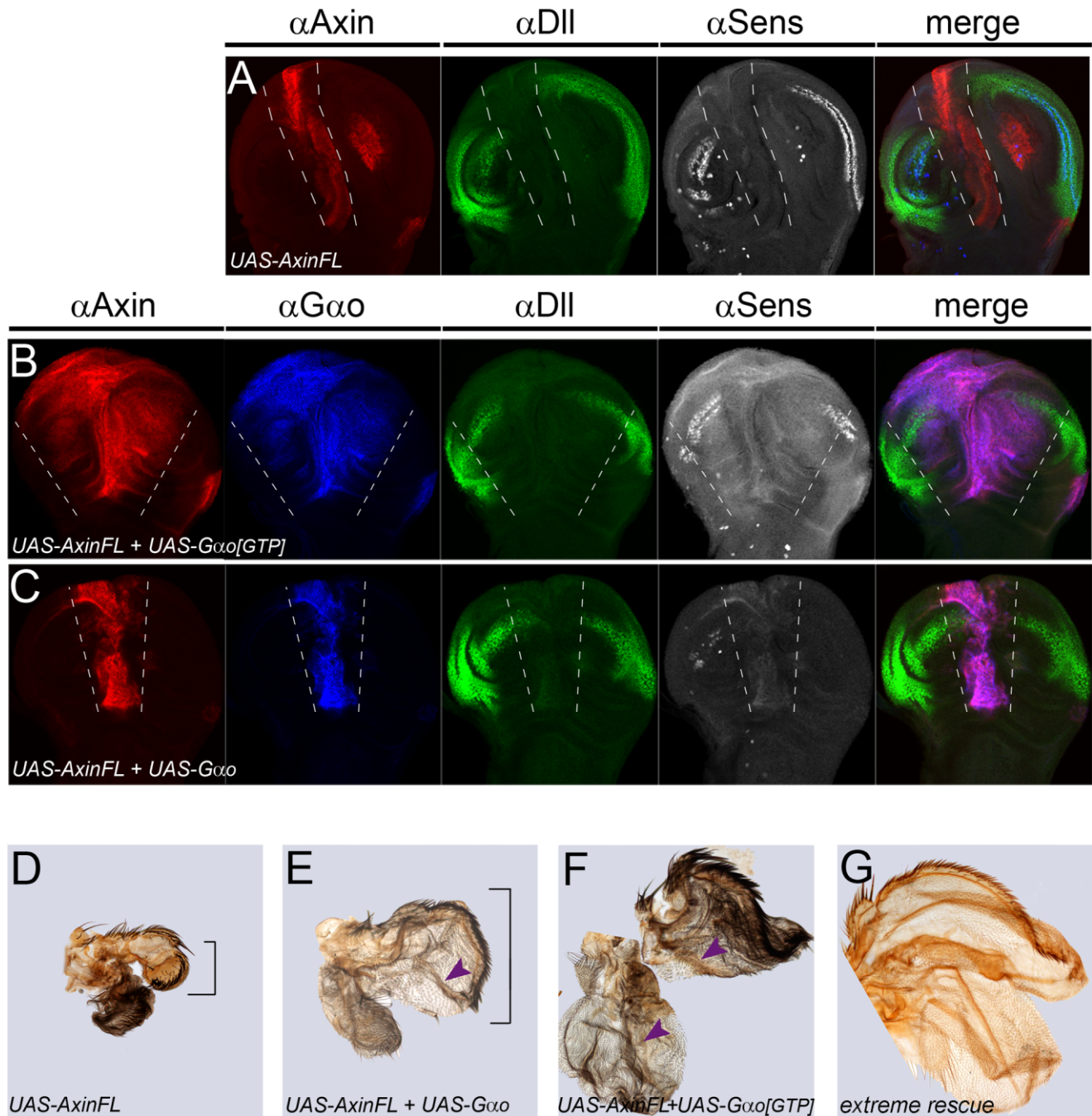


**Fig. 4.** Gαo can suppress inhibition of the Wnt pathway induced by Axin over-expression. **A–C:** Wing imaginal discs over-expressing either AxinFL alone (A), or together with Gαo[GTP] (B) or Gαo (C) stained with anti-Axin (red), anti-Gαo (blue), anti-DII (green), and anti-Sens (grey) antibodies. Gαo[GTP] and Gαo produce a different rescue of the size of the *omb-Gal4* region and DII and Sens expression in the AxinFL zone (marked by dashed lines). **D–F:** Adult wings with the same genotypes as in A–C. Wing size, margin (brackets), and vein (arrowheads) formation are significantly rescued by Gαo (E) and Gαo[GTP] (F). **G:** A wing from an *omb-Gal4*; *UAS-Gαo/UAS-AxinFL* fly showing extreme rescue.

### The $\beta\gamma$ -Subunits of the Trimeric Go Protein Physically Bind and Re-Localize Dsh

The results described above show that the GDP-loaded forms of Gαo, when expressed in the presence of AxinΔRGS,

dramatically impair Wnt signal transduction in the wing imaginal disc. Gα-subunits interact with the  $\beta\gamma$ -heterodimer only in the GDP-bound state (Gilman, 1987). We have also shown that the GDP-loaded forms of Gαo can compete for the  $\beta\gamma$ -subunits with the Gαs protein during wing maturation

(Katanayeva et al., unpublished data). We thus hypothesized that sequestration of the  $\beta\gamma$ -subunits by Gαo and Gαo[GDP] was the reason for the aggravation of the AxinΔRGS phenotypes.

Dsh is a cytoplasmic protein recruited to the plasma membrane upon activation of the Wnt pathway (Yana-



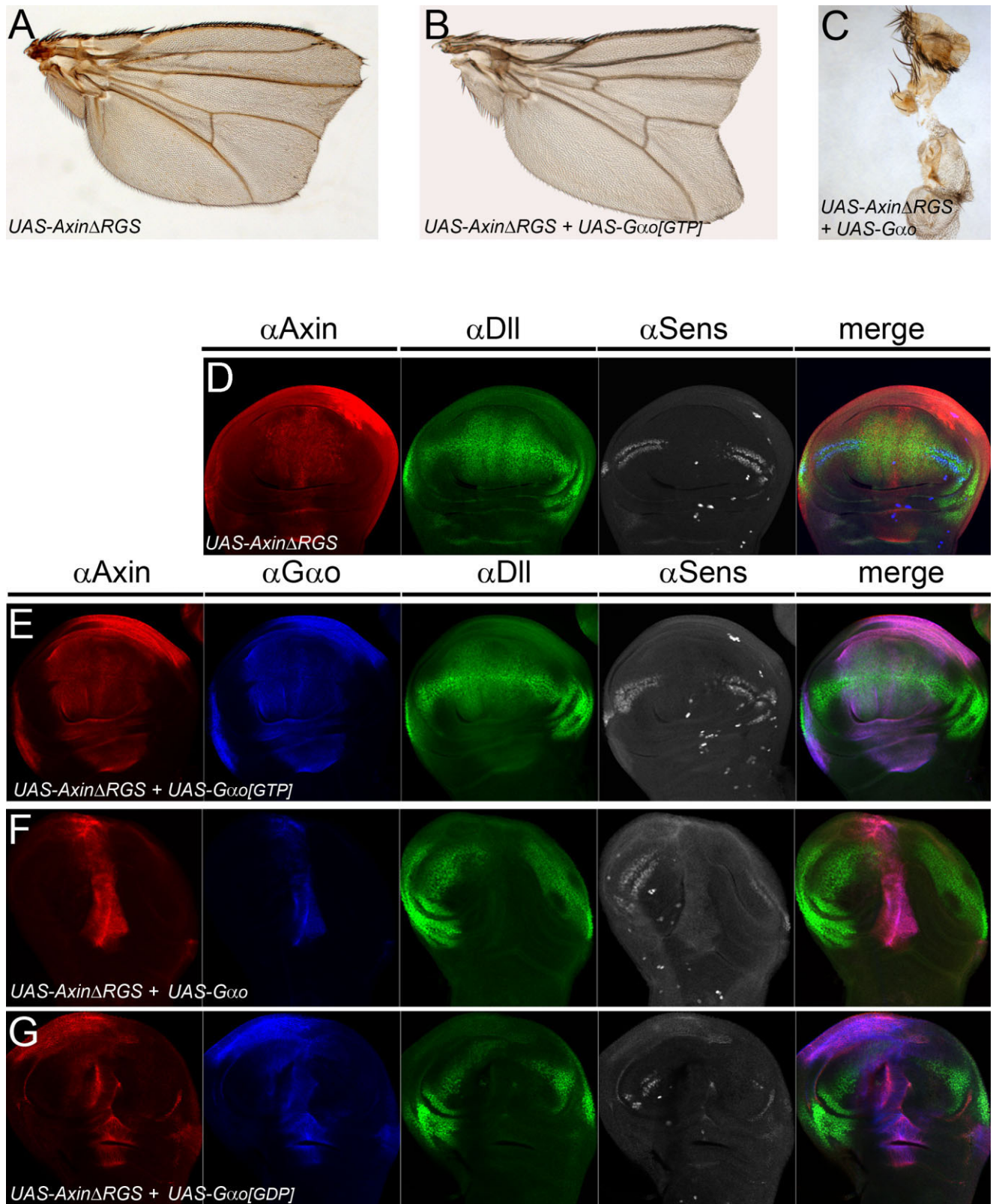


**Fig. 5.** The ability of G $\alpha$  to suppress Axin phenotypes requires Axin's RGS domain. Adult wings (A–C) and wing imaginal discs (D–G) expressing Axin $\Delta$ RGS alone (A, D) or together with different forms of G $\alpha$  show no suppression of the Axin $\Delta$ RGS phenotype by G $\alpha$ [GTP] (B, E) and a severe enhancement of the phenotype by G $\alpha$  (C, F) or G $\alpha$ [GDP] (G). Panel labelling is the same as on Figure 4.

gawa et al., 1995; Schwarz-Romond et al., 2007; Yokoyama et al., 2007). The direct interaction of Dsh with Axin through the heterodimerization of their DIX domains has been shown to contribute to the dissociation of the Axin-based  $\beta$ -catenin destruction complex (Cliffe et al., 2003; Schwarz-Romond et al., 2007). A direct binding of the  $\beta\gamma$ -subunits of trimeric G proteins to Dsh has been demonstrated for mammalian proteins (Angers et al., 2006; Jung et al., 2009). As the  $\beta\gamma$ -heterodimer is exclusively membrane-bound through strong lipid modification of the  $\gamma$ -subunit (Wedegaertner et al., 1995), we hypothesized that the  $\beta\gamma$  released from the trimeric Go protein could be required for Dsh recruitment from the cytoplasm to the plasma membrane upon Fz receptor activation.

To investigate this possibility, we first assayed the possible physical interaction of the *Drosophila* Dsh protein with the  $\beta\gamma$ -subunits. To obtain high amounts of pure and correctly modified  $\beta\gamma$ , we isolated G $\beta\gamma$  from pig brains by the conventional protocol (Northup et al., 1983; Sternweis and Robishaw, 1984); *Drosophila* Dsh was recombinantly expressed in *Escherichia coli* as an MBP-fusion protein. In accordance with the previously described interactions of mammalian Dsh with G $\beta\gamma$  (Angers et al., 2006; Jung et al., 2009), we found that G $\beta\gamma$  could be pulled-down by the *Drosophila* Dsh but not by the control protein MBP (Fig. 6A).

Next, to test the cellular consequence of such physical binding, we expressed the functional GFP-tagged version of Dsh (Axelrod, 2001) in the salivary glands, alone or together with G $\beta$ 13F or G $\beta$ 13F/G $\gamma$ 1 (the main G $\beta\gamma$ -subunits of *Drosophila*). When expressed alone, Dsh-GFP mainly stayed cytoplasmic with a weak plasma membrane staining (Fig. 6B, C), consistent with the lack of Wnt signaling in salivary gland cells of this larval stage (Li and White, 2003; de la Roche and Bienz, 2007). The cytoplasmic localization of Dsh-GFP became exclusive when G $\beta$ 13F was co-expressed with it (Fig. 6E, F). G $\beta$ -subunits do not carry lipid modifications (Wedegaertner et al., 1995). Thus, without co-expressed  $\gamma$ -subunit, G $\beta$ 13F

is cytoplasmic (Fig. 6D) and traps all Dsh in the cytoplasm.

In contrast, if G $\beta$ 13F and G $\gamma$ 1 were co-expressed, G $\beta$ 13F became plasma membrane-localized (Fig. 6G). Remarkably, co-expression of G $\beta$ 13F/G $\gamma$ 1 also recruited Dsh-GFP to the plasma membrane (Fig. 6H, I). Thus, targeted localization of the G $\beta$ 13F-subunit to the cytoplasm or the plasma membrane reciprocally re-localizes Dsh. The plasma membrane localization of Dsh forced by G $\beta$ 13F/G $\gamma$ 1 is similar to that induced by activation of the Wnt signaling in other cells (Yanagawa et al., 1995; Schwarz-Romond et al., 2007).

We also tested if G $\alpha$ o could re-localize Dsh in salivary glands. No re-localization of Dsh-GFP could be seen upon expression of G $\alpha$ o[GTP] (Supp. Fig. S1A, which is available online), but a partial re-localization could be observed upon expression of the wild-type form of G $\alpha$ o (Supp. Fig. S1B). However, G $\alpha$ o in any guanine nucleotide form failed to reveal any direct binding to Dsh (Supp. Fig. S1C). Thus, the direct interaction with Dsh appears to be specific for the G $\beta\gamma$  component of the trimeric Go protein. In another control of specificity, we found no ability of G $\beta\gamma$  to re-localize Axin-GFP in the salivary glands (Supp. Fig. S1D).

Our results demonstrate that the  $\beta\gamma$ -subunits can physically bind and recruit *Drosophila* Dsh, which might be important for the Wnt signaling, e.g., through the Dsh-mediated dissociation of the Axin-based destruction complex.

### Involvement of the $\beta\gamma$ -Subunits in the Wnt Signaling in *Drosophila* Wing

The results presented in the previous sections suggested that G $\beta\gamma$  could be involved in the Wnt signal transduction, directly acting on Dsh and indirectly acting on Axin. To test whether G $\beta\gamma$  was indeed required for the Wnt signaling, we expressed the UAS-RNAi constructs (Dietzl et al., 2007) targeting G $\beta$ 13F and/or G $\gamma$ 1 in the *Drosophila* wings. We initially used the *omb-Gal4* driver line used in the previous sections. Down-regulation of G $\beta$ 13F performed in this manner re-

sulted in formation of generally malformed crumpled wings with the appearance of long proximal hinge-type bristles in the base of the adult wing pouch together with the general expansion of the hinge region (data not shown). These phenotypes may indicate down-regulation of the Wnt signaling (Azpiazu and Morata, 2000).

To achieve a finer analysis of the possible function of G $\beta\gamma$  in the wing Wnt signaling, we expressed the RNAi constructs targeting G $\beta$ 13F and/or G $\gamma$ 1 (Dietzl et al., 2007) using the *hedgehog-Gal4* (*hh-Gal4*) driver, which produced strong expression in the posterior half of the wing, which allowed a direct comparison of the affected region to the control anterior part in the same tissue (Katanaev et al., 2005). Such down-regulation of G $\beta$ 13F in the posterior domain resulted in malformed adult wings losing the wing margin structures specifically in the *hh-Gal4*-expressing region (Fig. 7A), indicating loss of Wnt signaling. Additionally, long proximal hinge-type bristles could again be seen forming in

**Fig. 6.** G $\beta\gamma$  can directly bind and re-localize Dsh. **A:** In pull-down experiments, MBP-Dsh ("PD MBP-Dsh") but not MBP ("PD-MBP") is able to precipitate purified G $\beta\gamma$ . **B–I:** Salivary glands expressing Dsh-GFP alone (**B, C**) or together with UAS-G $\beta$ 13F (**D–F**) and UAS-G $\gamma$ 1 (**H, I**) were stained with antibodies to G $\beta$ 13F (red), GFP (green), and with DAPI (blue). Over-expression of G $\beta$ 13F leads to its exclusive cytoplasmic localization with identical diffuse appearance of Dsh-GFP (**D–F**). Co-overexpression of UAS-G $\beta$ 13F and UAS-G $\gamma$ 1 leads to a plasma membrane localization of G $\beta$ 13F and similar re-localization of Dsh-GFP (**H, I**).

**Fig. 7.** G $\beta\gamma$  is involved in the Wnt signaling in *Drosophila*. **A:** Down-regulation of G $\beta$ 13F by posteriorly expressed RNAi leads to loss of the wing margin (bracket) and appearance of proximal hinge-type bristles (arrowheads) in the posterior adult wing. **B, C:** In wing discs, down-regulation of G $\beta$ 13F leads to reduction in Sens (**B'**) and Cut expression (**C'**) in the posterior expression domain (arrows); Dll is not affected (**C**). The discs are oriented posterior to the right; anti-Hh staining is used to visualize the A/P border (marked with a thin line). **D, E:** Over-expression of G $\beta$ 13F alone (**D**) or together with G $\gamma$ 1 (**E**) in the posterior domain leads to loss of the posterior wing margin structures (**D, E**), and loss of Sens expression (**D', E'**). Dll expression is reduced in UAS-G $\beta$ 13F (**D''**), but not affected in UAS-G $\beta$ 13F; UAS-G $\gamma$ 1 (**E'**). The borders of the posterior domain are marked with small arrows.



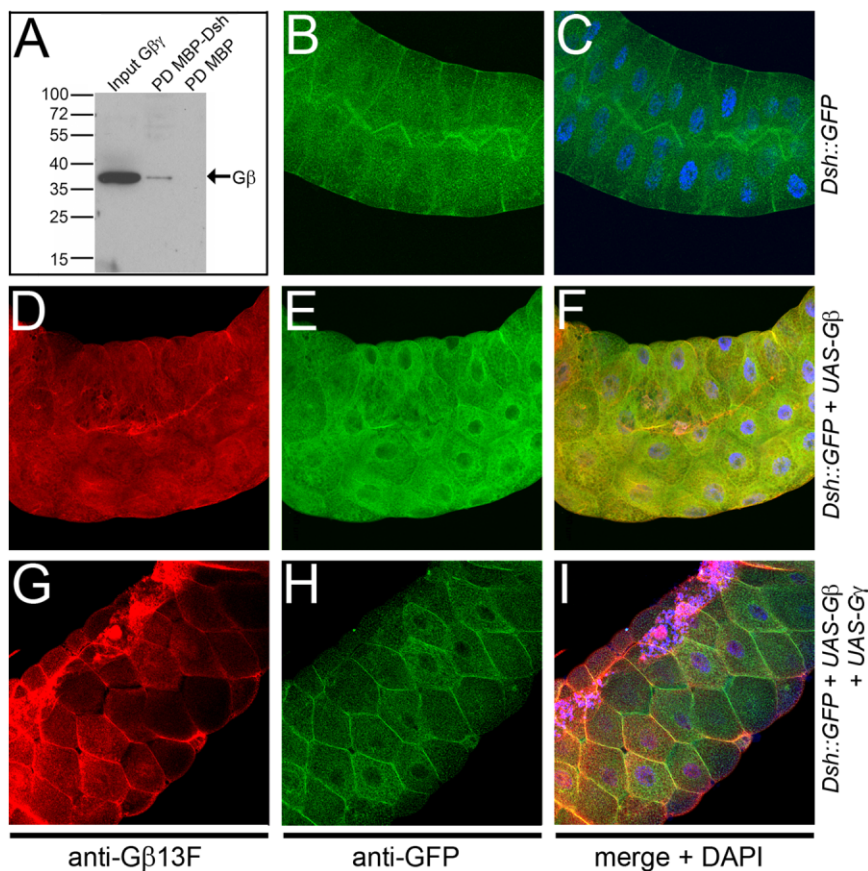
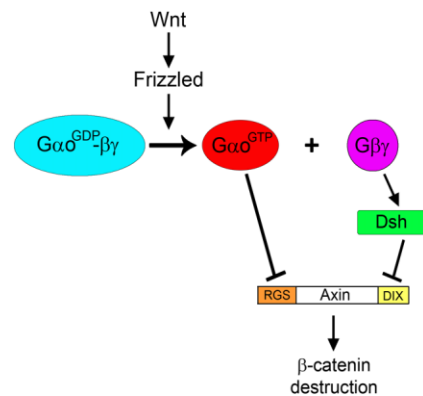


Fig. 6.



**Fig. 8.** A model of the early signaling events in Wnt signal propagation. Wnt ligand binding makes the Frizzled receptor competent to serve as a guanine nucleotide exchange factor towards the trimeric Go complex (Gα<sup>GDP</sup>-βγ), leading to dissociation of the complex into Gα<sup>GTP</sup> and Gβγ. Gα<sup>GTP</sup> directly inhibits Axin through the RGS domain of the latter. Gβγ recruits Dsh from the cytoplasm to the plasma membrane. The activated Dsh acts on Axin through the DIX domain. This double activity of the trimeric Go protein on Axin ensures the efficient inhibition of the latter, allowing β-catenin stabilization.

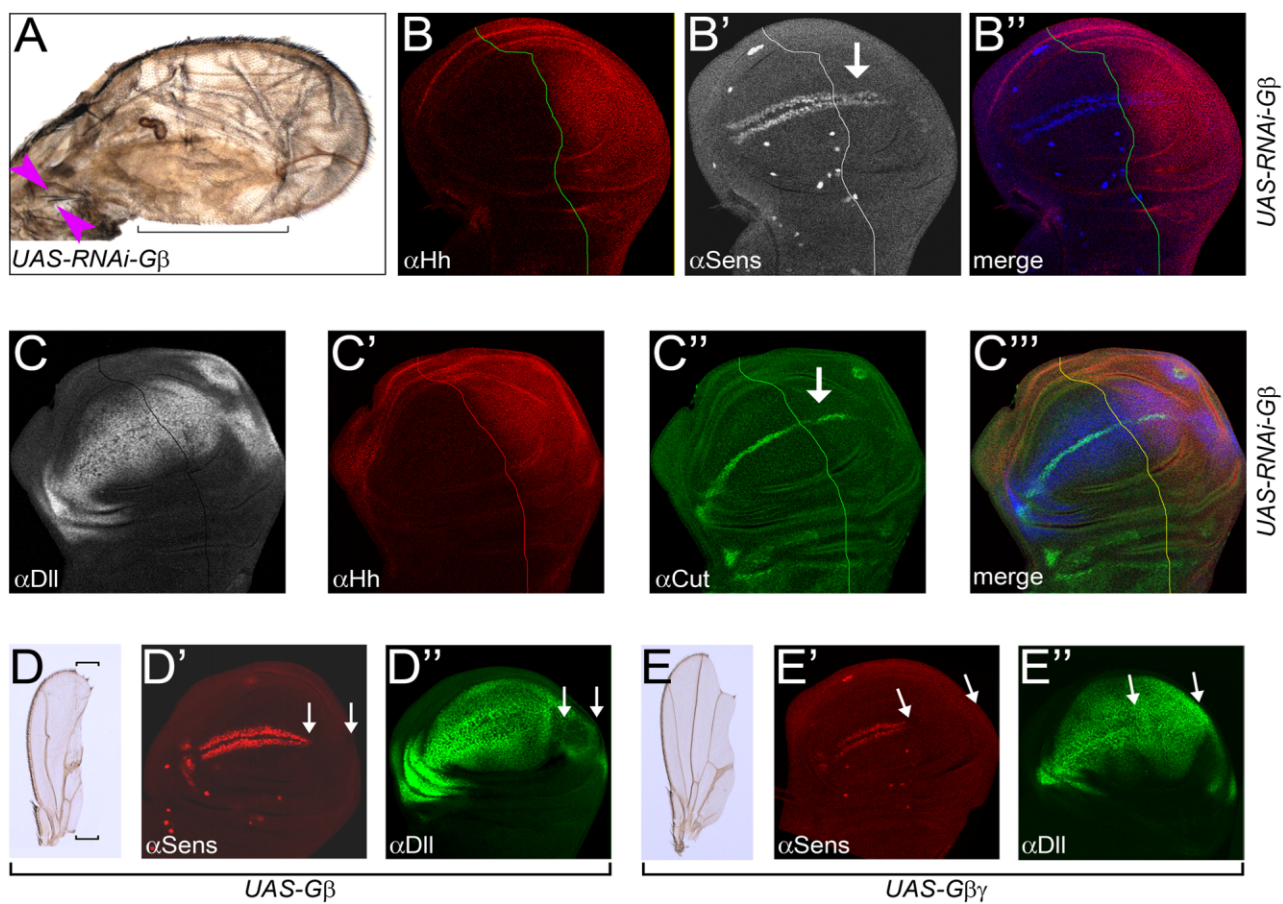


Fig. 7.

the targeted region (arrowheads in Fig. 7A).

Analysis of expression of the Wnt target genes in wing imaginal discs with down-regulated G $\beta$ 13F revealed a reduction in the expression of the short-range Wnt target Sens (Fig. 7B'); this reduction was more pronounced towards the proximal part of the future wing. Cut is another Wnt short-range target gene (Neumann and Cohen, 1996; Katanaev et al., 2005) and became similarly decreased upon G $\beta$ 13F down-regulation (Fig. 7C"). In contrast, expression of the long-range target gene Dll was not affected in these discs (Fig. 7C). These data demonstrate a function of the G $\beta$  $\gamma$  subunits in the transduction of the high-levels of Wnt signal in *Drosophila* wing.

In the salivary glands, over-expression of G $\beta$ 13F without its G $\gamma$ -partner resulted in accumulation of G $\beta$ 13F in the cytoplasm and trapping of Dsh away from the plasma membrane (Fig. 6D, E). We hypothesized that the similar over-expression of G $\beta$ 13F alone in wings might lead to the dominant inhibition of the Wnt pathway. To test this possibility, we over-expressed G $\beta$ 13F using the *hh-Gal4* driver. Remarkably, this resulted in severe Wnt loss-of-function phenotypes seen both in adult wings and in wing discs. In the adult wings, a complete loss of the posterior margin structures was induced, accompanied by a severe reduction in the size of the posterior region (Fig. 7D). As expected, these phenotypes were paralleled by a severe growth defect of the affected region with a complete loss of Sens (Fig. 7D') and Cut (not shown), and a decrease in the expression of Dll (Fig. 7D").

However, we also expected that a co-overexpression of G $\beta$ 13F and G $\gamma$ 1 in the wing discs would lead to the over-activation of the Wnt pathway. In contrast, we again found a down-regulation of the Wnt signaling, albeit at lower levels as compared to those of over-expression of G $\beta$ 13F alone. Specifically, adult wings were losing the wing margin but rarely had a reduction in the size of the posterior domain (Fig. 7E). Similarly, the size of the posterior region was mostly normal in wing discs and typically did not show

a decrease in Dll staining, yet Sens expression was lost (Fig. 7E', E").

The possible explanation of these phenotypes, as well as the model for the interplay between G $\alpha$ o, G $\beta$  $\gamma$ , Dsh, and Axin are further elaborated in the Discussion section.

## DISCUSSION

We have demonstrated that G $\alpha$ o can physically bind the RGS domain of Axin and recruit it to the plasma membrane, the action likely leading to the destabilization of the Axin-based  $\beta$ -catenin destruction complex and propagation of the Wnt signal inside the cell. In support of this idea, we have shown that G $\alpha$ o can suppress the Wnt loss-of-function phenotypes induced by Axin over-expression in wing imaginal discs. This rescue critically depends on the presence of the RGS domain, reiterating the crucial role of this domain for the interaction with G $\alpha$ o. While the GTP-bound form of G $\alpha$ o is unable to change the phenotypes of the Axin $\Delta$ RGS expression, the GDP-bound forms of G $\alpha$ o even dramatically enhance these phenotypes. We hypothesize that this enhancement is due to sequestration of the G $\beta$  $\gamma$  heterodimer by the GDP-forms of G $\alpha$ o. We also show that G $\beta$  $\gamma$  can directly bind and recruit Dsh from the cytoplasm to the plasma membrane, thus possibly contributing to the propagation of the Wnt signal.

The RGS domain of Axin, responsible for the interaction with G $\alpha$ o, is important for the full range of Axin activity in wing imaginal discs. Indeed, over-expression of the  $\Delta$ RGS form of Axin only partially suppresses Wnt signaling in this tissue (Fig. 3). The RGS domain of Axin is known to bind APC, another component of the  $\beta$ -catenin-destruction complex (Behrens et al., 1998; Hart et al., 1998; Kishida et al., 1998; Nakamura et al., 1998). The inability of Axin $\Delta$ RGS to directly interact with APC is the likely reason for the reduced activity of this construct in *Drosophila* wings (Fig. 3) and in vertebrates (Zeng et al., 1997; Fagotto et al., 1999; Chia et al., 2009). The G $\alpha$ o and G $\alpha$ q proteins were shown to dissociate the Axin-based destruction complexes in mammalian cells (Liu et al., 2005). We propose that in *Drosophila*, G $\alpha$ o leads to a sim-

ilar dissociation of the destruction complex through direct binding to the RGS domain of Axin, which recruits Axin to the plasma membrane (Fig. 1) and probably displaces APC from Axin.

In vitro, the purified RGS domain of Axin binds equally well both the GDP- and the GTP-loaded forms of G $\alpha$ o (Fig. 2). It also lacks the GTPase-activating protein (GAP) activity towards G $\alpha$ o, typical for other RGS domains. These data agree with the absence of some of the conserved residues required for the GAP action in Axin RGS (Zeng et al., 1997). Thus, biochemically Axin binds G $\alpha$ o regardless of its nucleotide form. However, in vivo the GDP- and the GTP-loaded forms of G $\alpha$ o behave differently towards Axin. Only G $\alpha$ o[GTP] is capable of recruiting Axin-GFP to the plasma membrane in the salivary glands (Fig. 1). Similarly, G $\alpha$ o[GTP] is much more potent in rescuing the Axin full-length over-expression effects in wing imaginal discs and adult wings (Fig. 4). This seeming contradiction is explained by the fact that in vivo the GDP-loaded forms of G $\alpha$ o bind the  $\beta$  $\gamma$ -subunits, recreating the trimeric Go complexes. Indeed, over-expressed, the wild-type G $\alpha$ o was shown to compete with other G $\alpha$  proteins for the  $\beta$  $\gamma$ -subunits (Katanaev et al., unpublished data). Only the G $\alpha$ o[GTP] form can stay free and thus exert its activities on Axin in full.

On the other hand, the wild-type G $\alpha$ o also possesses a capacity of over-activating the Wnt pathway in wing imaginal discs (Katanaev et al., 2005), and can to a certain degree rescue the phenotypes of Axin over-expression in this tissue (Fig. 4). This contrasts with its inability to recruit Axin-GFP to the plasma membrane in salivary glands (Fig. 1). These differences between the two tissues correlate with the degree of Wnt signal transduction. Indeed, the Wnt pathway is highly active in the wing imaginal discs, and G $\alpha$ o can further enhance the pathway relying on the activity of Fz receptors (Katanaev et al., 2005). In contrast, in larval salivary glands the Wnt pathway is silent (Li and White, 2003; de la Roche and Bienz, 2007), which is illustrated by the cytoplasmic localization of Dsh in this tissue (Fig. 6), expected to be plasma membrane localized when the pathway is on (Yanagawa et al., 1995).



It thus seems probable that in the salivary glands  $G\alpha o$ , forming trimeric Go complexes with  $G\beta\gamma$ , fails to be further converted into the monomeric form due to the absence of the Wnt/Fz activity. In contrast, wing imaginal discs provide enough Wnt/Fz activity to activate endogenous as well as exogenous Go, which can then recruit Axin and thus propagate the signal.

The ability of the GDP-bound forms of  $G\alpha o$  to bind to the  $\beta\gamma$ -subunits is the likely reason for the aggravation of the Axin $\Delta$ RGS phenotype induced by  $G\alpha o$ . This form, even upon conversion to the GTP-bound state by the action of the Wnt/Fz complexes, can no longer bind the RGS-lacking Axin and suppress Axin's negative action on the Wnt signal transduction. However, it can bind  $G\beta\gamma$ . We propose that  $G\beta\gamma$  plays, in addition to  $G\alpha o$ -GTP, a positive role in the Wnt signal transduction through its ability to bind and recruit Dsh to the plasma membrane. Over-expression of  $G\alpha o$  reduces the amounts of free  $G\beta\gamma$ , reducing the efficiency of Dsh re-localization. We propose that when the endogenous full-length Axin is present, over-expression of  $G\alpha o$  has the overall stimulating effect on the Wnt signaling in wing discs (Katanaev et al., 2005) due to increased generation of  $G\alpha o$ -GTP, which binds and antagonizes Axin. It is only in the artificial situation of over-expression of Axin $\Delta$ RGS that the other, negative, effect of  $G\alpha o$  can be revealed. To prove that  $G\alpha o$  aggravates the Axin $\Delta$ RGS phenotypes due to sequestration of  $G\beta\gamma$ , we tested the mutant  $G\alpha o$ [GDP] protein unable to charge with GTP (Katanaev et al., 2005) but still capable to bind  $G\beta\gamma$  (Inoue et al., 1995) and found that this form was similar to  $G\alpha o$  in enhancing the Axin $\Delta$ RGS phenotypes (Fig. 5).

We have performed direct experiments testing the involvement of  $G\beta\gamma$  in Wnt signaling. In accordance with our predictions, down-regulation of  $G\beta\gamma$  results in a clear reduction of the Wnt signaling in *Drosophila* wings and wing discs, affecting the short-range target genes of the Wnt pathway (Fig. 7). As over-expression of  $G\beta$  alone leads to trapping Dsh in the cytoplasm (Fig. 6E), such over-expression also produces drastic dominant effects on Wnt signaling in wing discs (Fig. 7D). Unfortunately, we were un-

able to confirm that Dsh was trapped in the cytoplasm of the epithelial cells of such discs due to the low resolution of the Dsh staining we obtained in these thin columnar cells. Additionally, not only localization but also abundance of the components of the Wnt pathway are known to change in cells with high levels of Fz activation as part of the feedback regulation (Tolwinski and Wieschaus, 2004; Itoh et al., 2005; Angers et al., 2006; Yokoyama et al., 2007; Jung et al., 2009). Thus, interpretation of Dsh localization in wing imaginal discs upon perturbations of the Wnt pathway will be difficult. Instead, analysis of a tissue where the Wnt pathway is endogenously silent, such as salivary glands (Li and White, 2003; de la Roche and Bienz, 2007), allows analysis of the direct influence of the subunits of the trimeric Go complex on cellular localization of the components of the Wnt pathway. This analysis let us identify the plasma membrane re-localization of Axin by  $G\alpha o$  and of Dsh by  $G\beta\gamma$  as such direct cellular responses. These primary responses are probably then utilized in the physiological context as the basis to build positive and negative feedbacks for the final outcome of Wnt signal propagation.

While the numerous data discussed above indicate that  $G\beta\gamma$  is necessary for the proper activation of the Wnt pathway, probably through plasma membrane re-localization of Dsh, we could not over-activate the Wnt pathway by over-expression of  $G\beta$  and  $G\gamma$  together. Instead, the pathway was down-regulated, although to a weaker extent than that seen by over-expression of  $G\beta$  alone (Fig. 7E). This observation is not easy to reconcile with our other data. One possible explanation is that in the wing discs, unlike the salivary glands, co-overexpression of  $G\gamma$  might be insufficient to attract the complete pool of  $G\beta$  to the plasma membrane, and significant amounts of  $G\beta$  may still remain cytoplasmic and retain Dsh. Along these lines, co-overexpression of  $G\gamma$  shows a partial "rescue" of the phenotypes induced by  $G\beta$  over-expression (Fig. 7D, E). Another possible explanation involves the notion of the negative feedback regulation in the Wnt cascade. Proteosomal degradation of Dsh during Wnt signal transduction has been demonstrated

(Angers et al., 2006). A recent work has shown that targeted plasma membrane localization of Dsh by the Wnt activation or by the  $G\beta\gamma$  subunits also destines it for the lysosomal degradation in vertebrate cells (Jung et al., 2009). Thus, the activity of  $G\beta\gamma$  in the Wnt signaling may be multistep: the initial recruitment of Dsh from the cytosol may serve to activate the pathway, but the persistent membrane localization will lead to Dsh degradation. While  $G\beta$  RNAi targeting shows that the  $G\beta\gamma$  complex is necessary for the proper Wnt signaling, activation of such a negative feedback loop may underlie the phenotypes we observe upon the persistent over-expression of  $G\beta\gamma$ . In this scenario,  $G\beta\gamma$  will be added to the growing list of regulators of the Wnt pathway, which have both positive and negative activities in this signaling (Davidson et al., 2005; Zeng et al., 2005; Takacs et al., 2008).

We favor the model whereby  $G\beta\gamma$  induce plasma membrane re-localization of Dsh serves as an initial positive impact to activate the Wnt signal propagation. If this is correct, what may be the immediate consequences of the  $G\beta\gamma$ -induced plasma membrane recruitment of Dsh? This scaffolding protein is known to become hyperphosphorylated upon plasma membrane localization, which correlates with its activity in the Wnt signal transduction (Yanagawa et al., 1995). Dsh is known to directly bind Axin through the DIX domain heterodimerization (Cliffe et al., 2003; Schwarz-Romond et al., 2007). Although a direct interaction of  $G\beta\gamma$  with Axin's protein phosphatase 2A-binding region (N-terminal to the DIX domain) has recently been demonstrated in mammalian cells (Jung et al., 2009), we found no ability of  $G\beta\gamma$  to re-localize or directly bind *Drosophila* Axin (Supp. Fig. S1D and data not shown). Overall, our data and the above considerations let us propose the following model of the action of the trimeric Go protein in the *Drosophila* Wnt/Fz pathway (Fig. 8).

The trimeric Go protein is a direct target of the activated Fz receptors (Malbon, 2005; Egger-Adam and Katanaev, 2008). Wnt ligand binding to Fz activates the guanine nucleotide exchange activity of Fz towards Go (Katanaev et al., 2005; Katanaev and

Buestorf, 2009). This in turn dissociates the trimeric Go complex into G $\alpha$ -GTP and G $\beta\gamma$ . We propose that both these components of the trimeric complex have the initial positive activity in Wnt signal propagation (Fig. 8). G $\alpha$ -GTP directly binds to the RGS domain of Axin, recruiting Axin to the plasma membrane and dissociating the Axin-based  $\beta$ -catenin destruction complex. On the other hand, G $\beta\gamma$  recruits and contributes to activation of Dsh, which then can bind the DIX domain of Axin and thus also promote dissociation of the destruction complex. These two branches of G protein-mediated signal propagation converge on the Axin complex to cooperatively ensure its efficient inhibition (Fig. 8). Such a double effect on Axin emanating from the trimeric Go complex may serve to ensure a robust activation of the Wnt signaling.

## EXPERIMENTAL PROCEDURES

### Fly Stocks

*omb-Gal4* (Lecuit et al., 1996); *hh-Gal4* (Tanimoto et al., 2000); *71B-Gal4* and *GMR-Gal4* (Bloomington Drosophila Stock Center); *UAS-AxinFL*, *UAS-AxinFLmyc*, *UAS-Axin $\Delta$ RGSmyc* (Willert et al., 1999); *UAS-Go<sup>wt</sup>*, *UAS-Go<sup>GTP</sup>*, *UAS-Go<sup>GDP</sup>* (Katanaev et al., 2005); *UAS-G $\beta$ 13F* (Katanaev and Tomlinson, 2006); *UAS-G $\gamma$ 1* (Izumi et al., 2004); *UAS-RNAi-G $\beta$ 13F* and *UAS-RNAi-G $\gamma$ 1* (Vienna Drosophila RNAi Center); *UAS-AxinGFP* (Cliffe et al., 2003); *dsh::GFP* (Axelrod, 2001). All images of the *omb-Gal4*; *UAS-Axin* phenotypes are from female flies/larvae. The *UAS-AxinFL* and *UAS-Axin $\Delta$ RGSmyc* stocks produce similar Axin expression, while *UAS-AxinFLmyc* gives lower expression levels.

### Histology

Adult fly wings and wing imaginal discs were prepared as in Katanaev et al. (2005); wing discs were mounted in Moviol. Salivary glands were dissected in 0.9% NaCl, fixed in 3.7% Formaldehyde/PBS, permeabilized in 0.5% NP40/PBS for 30 min, washed three times with PBS, and then preincubated in 0.2% Tween 20/PBS

(PBT) for 10 min. The first antibody was added in PBT and incubated for 2 hr at RT followed by three times washing with PBT. The secondary antibody in PBT was added together with DAPI for 2 hr followed by three final washing steps in PBT and mounting in Moviol.

Antibodies used: goat-anti-Axin at 1:10 (Santa Cruz cat. No. sc-15685); guinea pig anti-Dll at 1:1,000 (Estella and Mann, 2008) and anti-Sens at 1:1,000 (Nolo et al., 2000); mouse-anti-Dll at 1:1,000 (gift of G. Struhl), anti-GFP at 1:1,000 (Roche Diagnostics), and anti-Cut at 1:20 (Developmental Studies Hybridoma Bank); rabbit anti-Hh (NHhI) at 1:1,000 (Takei et al., 2004), anti-G $\alpha$  at 1:100 and anti-G $\beta\gamma$  at 1:1,000 (Calbiochem cat. nos. 371726 and 371821, respectively); rat anti-Dsh at 1:1,000 (Shimada et al., 2001). For DNA staining 4',6-Diamidin-2'-phenylindol- dihydrochlorid was used at 1:1,000 (DAPI; Roche).

### Cloning

The full-length *Drosophila* Axin ORF from pPac5.1-Axin (Cong and Varbus, 2004) was cloned into the pCR2.1-TOPO plasmid (Invitrogen) using the oligos: forward: GGGATC-CATGAGTGGCCATCCATC, and reverse: CTTAATCGGATGGCTTGA-CAAG, and subsequently cloned into the pQE31 plasmid (Qiagen) with HindIII and EcoRV for bacterial expression as an N-terminally His<sub>6</sub>-tagged protein. To obtain the pQE31-AxinRGS plasmid, pQE31-Axin was digested with AfeI (cutting at codon 180 of Axin ORF [RGS domain located at amino acids 51–172] and HindIII [located in pQE31 after the Axin ORF insert] and relegated. Full-length *Drosophila* Dsh open reading frame was cloned in pMAL-c2X (New England BioLabs) using the restriction enzymes BamHI and HindIII. The resulting *E. coli* expression protein is an N-terminally MBP-tagged fusion protein.

### Protein Expression

*E. coli* strain Top10 (Invitrogen) was freshly transformed with the pQE31-AxinRGS, pMAL-Dsh or pMAL-2X (New England BioLabs) plasmids for expression of His<sub>6</sub>-AxinRGS, MBP-

Dsh, or MBP (maltose binding protein). No expression of the full-length Axin could be obtained in bacteria. Transformed cells were grown at 37°C to the OD(600) = 0.6 before induction with 1 mM IPTG and additional growth for 4 hr at 37°C, followed by harvesting by centrifugation and storage at –20°C overnight. All subsequent steps were performed at 0–4°C. The His<sub>6</sub>-AxinRGS-expressing cell pellets were re-suspended in the lysis buffer (50 mM NaH<sub>2</sub>PO<sub>4</sub>; 300 mM NaCl; 10 mM imidazole; complete EGTA-free protease inhibitor cocktail (Roche); pH 8.0), destroyed by sonication 10 $\times$  for 15 sec and centrifuged for 30 min at 12,000 rpm to eliminate cell debris. The supernatant was added to Ni<sup>2+</sup>-agarose (Qiagen) pre-equilibrated with the lysis buffer and incubated for 1 hr at 4°C. The resin was then washed three times with the washing buffer (50 mM NaH<sub>2</sub>PO<sub>4</sub>; 300 mM NaCl; 20 mM imidazole; pH 8.0) and eluted with same buffer supplemented with 250 mM imidazole.

The MBP- or MBP-Dsh-expressing cell pellets were re-suspended in the column buffer (20 mM Tris, pH 7.4; 200 mM NaCl; 1 mM EDTA; 1 mM DTT). MBP and MBP-Dsh were purified as above except for the usage of amylose resin (New England BioLabs), pre-equilibrated and washed with the column buffer. Elution was achieved in same buffer supplemented with 10 mM maltose.

His<sub>6</sub>-tagged or non-tagged G $\alpha$  and G $\alpha$ [Q205L] were prepared as purified proteins or as bacterial lysates as described in (Kopein and Katanaev, 2009). To obtain myristoylated G proteins, non-tagged G $\alpha$  and G $\alpha$ [Q205L] were expressed in Top10 containing pBB131 expressing an *N*-myristoyl transferase (Duronio et al., 1990).

### Pull-Down and Western Blotting

AxinRGS or MBP were immobilized on CNBr sepharose (GE Healthcare) according to the manufacturer's instructions. Empty CNBr sepharose was prepared alongside by blocking all active groups with Tris. Fifty microliters of the 50% CNBr slurry was washed twice with HKB\* (135 mM KCl; 10 mM NaCl; 10 mM Hepes-



KOH pH 7.5; 2 mM EGTA; 1 mM DTT; 0.1% Tween 20; 5% Glycerol) before application of the *E. coli* lysate containing various overexpressed forms of G $\alpha$  or G $\alpha$ [Q205L] (His $_6$ -tagged or untagged, myristoylated or not). Identical molar amounts of the various added forms of G $\alpha$  were ensured through anti-G $\alpha$  Western blots. The slurries were incubated for 3 hr at 4°C on a rotary shaker and washed 8× with 1 ml HKB\* for the total of 25 min before addition to the drained matrix of 50  $\mu$ l 2×SDS loading buffer and 5-min boiling. The samples were resolved on 10% SDS-PAGE followed by Western blotting. The competition experiments were performed adding soluble RGS protein to the 7.5-fold molar excess over the RGS immobilized on sepharose.

For experiments with the purified His $_6$ -G $\alpha$ , the G protein was preloaded prior to pull-down with 1 mM GTP $\gamma$ S or GDP for 1 hr at RT in 135 mM KCl; 10 mM NaCl; 25 mM MgCl $_2$ ; 10 mM Hepes-KOH pH 7.5; 2 mM EGTA; 1 mM DTT. Loading efficiency was independently controlled as in Kopein and Katanaev (2009).

To compare expression levels of different *UAS-Axin* constructs, salivary glands of the *71B-Gal4; UAS-Axin* 3rd instar larvae were dissected in 0.9% NaCl, which was next exchanged with the insect-lysis buffer (150 mM NaCl; 50 mM Tris pH 8.0; 1% Triton X-100; protease inhibitor cocktail; Roche) in proportion to 50  $\mu$ l per approximately 20 salivary gland pairs. The same amount of proteins (measured by Bradford) was used for the Western blot. Afterward, the Western blot membranes were stained with Coomassie Brilliant Blue R250 (Fluka).

For the G $\beta\gamma$  pull-down experiments, equal molar amounts of MBP-Dsh or MBP were added to pig G $\beta\gamma$  (purified as described by Northup et al., 1983; Sternweis and Robishaw, 1984) in the G $\beta\gamma$  buffer (50 mM Hepes, pH 7.5; 150 mM NaCl; 1 mM EDTA; 1 mM DTT; 0.1% Lubrol PX) and incubated for 1 hr 30 min at 17°C. The protein mix was then added to 50  $\mu$ l amylose resin pre-equilibrated in the G $\beta\gamma$  buffer, followed by an additional 1 hr 30 min incubation at 17°C. The resin was washed 4 times for 40 min with the G $\beta\gamma$  buffer and then the proteins were

eluted with the same buffer supplemented with 10 mM maltose.

Multiple experiments testing a possible interaction of Dsh with G $\alpha$  were performed. These included: (1) experiments with MBP-Dsh (or MBP alone) interacting with recombinant G $\alpha$  or G $\alpha$ [GTP] provided as bacterial lysates or as purified His $_6$ -fusions essentially as the experiments described for Axin above (Fig. 2A–D); (2) pull-downs of G $\alpha$  purified from pig brains in a manner similar to that shown with G $\beta\gamma$  in Figure 6A; (3) pull-downs of endogenous *Drosophila* G $\alpha$  from extracts of flies over-expressing G $\alpha$  or G $\alpha$ [GTP]. Under no conditions could we see a physical binding of Dsh to G $\alpha$ . The experiment of Supp. Fig. S1C depicts no interaction of recombinant Dsh with G $\alpha$  from head extracts of the *GMR-Gal4; UAS-G $\alpha$*  or *GMR-Gal4; UAS-G $\alpha$ [GTP]* flies; the experiment was performed under conditions that reveal a robust binding of *Drosophila* G $\alpha$  to the recombinant Pins protein (Kopein and Katanaev, 2009).

Antibodies used: goat-anti-Axin (Santa Cruz) at 1:100; rabbit-anti-G $\alpha$  (Calbiochem) at 1:1,000; mouse-anti-tubulin (clone E7, Developmental Studies Hybridoma Bank) at 1:500; rabbit-anti-G $\beta\gamma$  at 1:1,000 (Calbiochem cat. no. 371821).

### GTP Binding and Hydrolysis Assays

The GTP hydrolysis assay was performed according to Jameson et al. (2005) using 1  $\mu$ M His $_6$ -G $\alpha$ , 0.5  $\mu$ M BODIPY-GTP (Invitrogen) and the indicated concentrations of His $_6$ -Axin-RGS in 20 mM Tris pH 7.4; 1 mM EDTA; 10 mM MgCl $_2$ . Fluorescence measurements were performed with a PerkinElmer VICTOR3™ multiwell reader with excitation at 485 nm and emission at 530 nm at room temperature for 15 min. The GTP incorporation assay was performed according to McEwen et al. (2001) using 2  $\mu$ M His $_6$ -G $\alpha$  and 1  $\mu$ M BODIPY-GTP $\gamma$ S (Invitrogen). Measurements were done as above during 30 min.

### ACKNOWLEDGMENTS

We are grateful to Jeffrey Axelrod, Hugo Bellen, Jeffrey Gordon, Richard

Mann, Fumio Matsuzaki, Roel Nusse, Gary Struhl, Tetsuya Tabata, Tadashi Uemura, Harold Varmus, the Bloomington stock center, the Developmental Studies Hybridoma Bank, and the Vienna *Drosophila* RNAi Center for fly stocks, antibodies, and plasmids. We thank A. Koval, D. Kopein, V. Purvanov, N. Katagihallimath, S. Ziolek, and the whole Katanaev lab for discussions and materials. This work was funded by the Deutsche Forschungsgemeinschaft (TransRegio-SFB11) to V.L.K.

### REFERENCES

- Aberle H, Bauer A, Stappert J, Kispert A, Kemler R. 1997. beta-catenin is a target for the ubiquitin-proteasome pathway. *Embo J* 16:3797–3804.
- Angers S, Thorpe CJ, Biechele TL, Goldenberg SJ, Zheng N, MacCoss MJ, Moon RT. 2006. The KLHL12-Cullin-3 ubiquitin ligase negatively regulates the Wnt-beta-catenin pathway by targeting Dishevelled for degradation. *Nat Cell Biol* 8:348–357.
- Axelrod JD. 2001. Unipolar membrane association of Dishevelled mediates Frizzled planar cell polarity signaling. *Genes Dev* 15:1182–1187.
- Azpiaz N, Morata G. 2000. Function and regulation of homothorax in the wing imaginal disc of *Drosophila*. *Development* 127:2685–2693.
- Behrens J, Jerchow BA, Wurtele M, Grimm J, Asbrand C, Wirtz R, Kuhl M, Wedlich D, Birchmeier W. 1998. Functional interaction of an axin homolog, conductin, with beta-catenin, APC, and GSK3beta. *Science* 280:596–599.
- Castellone MD, Teramoto H, Williams BO, Druey KM, Gutkind JS. 2005. Prostaglandin E2 promotes colon cancer cell growth through a Gs-axin-beta-catenin signaling axis. *Science* 310:1504–1510.
- Chia IV, Kim MJ, Itoh K, Sokol SY, Costantini F. 2009. The RGS domain and the six C-terminal amino acids of mouse axin are both required for normal embryogenesis. *Genetics* 181:1359–1368.
- Cliffe A, Hamada F, Bienz M. 2003. A role of Dishevelled in relocating Axin to the plasma membrane during wingless signaling. *Curr Biol* 13:960–966.
- Cong F, Varmus H. 2004. Nuclear-cytoplasmic shuttling of Axin regulates subcellular localization of beta-catenin. *Proc Natl Acad Sci USA* 101:2882–2887.
- Davidson G, Wu W, Shen J, Bilic J, Fenger U, Stanek P, Glinka A, Niehrs C. 2005. Casein kinase 1 gamma couples Wnt receptor activation to cytoplasmic signal transduction. *Nature* 438:867–872.
- De Ferrari GV, Moon RT. 2006. The ups and downs of Wnt signaling in prevalent neurological disorders. *Oncogene* 25:7545–7553.
- de la Roche M, Bienz M. 2007. Wingless-independent association of Pygopus with

- dTCF target genes. *Curr Biol* 17:556–561.
- Dietzl G, Chen D, Schnorrer F, Su KC, Barinova Y, Fellner M, Gasser B, Kinsey K, Oppel S, Scheiblaue S, Couto A, Marra V, Keleman K, Dickson BJ. 2007. A genome-wide transgenic RNAi library for conditional gene inactivation in *Drosophila*. *Nature* 448:151–156.
- Dohlman HG, Thorner J. 1997. RGS proteins and signaling by heterotrimeric G proteins. *J Biol Chem* 272:3871–3874.
- Duronio RJ, Jackson-Machelski E, Heuckeroth RO, Olins PO, Devine CS, Yonemoto W, Slice LW, Taylor SS, Gordon JL. 1990. Protein N-myristoylation in *Escherichia coli*: reconstitution of a eukaryotic protein modification in bacteria. *Proc Natl Acad Sci USA* 87:1506–1510.
- Egger-Adam D, Katanaev VL. 2008. Trimeric G protein-dependent signaling by Frizzled receptors in animal development. *Front Biosci* 13:4740–4755.
- Estella C, Mann RS. 2008. Logic of Wg and Dpp induction of distal and medial fates in the *Drosophila* leg. *Development* 135:627–636.
- Fagotto F, Jho E, Zeng L, Kurth T, Joos T, Kaufmann C, Costantini F. 1999. Domains of axin involved in protein-protein interactions, Wnt pathway inhibition, and intracellular localization. *J Cell Biol* 145:741–756.
- Feigin ME, Malbon CC. 2007. RGS19 regulates Wnt-beta-catenin signaling through inactivation of G $\alpha$ (o). *J Cell Sci* 120:3404–3414.
- Fredriksson R, Lagerstrom MC, Lundin LG, Schioth HB. 2003. The G-protein-coupled receptors in the human genome form five main families. Phylogenetic analysis, paralogon groups, and fingerprints. *Mol Pharmacol* 63:1256–1272.
- Gilman AG. 1987. G proteins: transducers of receptor-generated signals. *Annu Rev Biochem* 56:615–649.
- Hart MJ, de los Santos R, Albert IN, Rubinfeld B, Polakis P. 1998. Downregulation of beta-catenin by human Axin and its association with the APC tumor suppressor, beta-catenin and GSK3 beta. *Curr Biol* 8:573–581.
- He X, Semenov M, Tamai K, Zeng X. 2004. LDL receptor-related proteins 5 and 6 in Wnt/beta-catenin signaling: arrows point the way. *Development* 131:1663–1677.
- Inoue S, Hoshino S, Kukimoto I, Ui M, Katada T. 1995. Purification and characterization of the G203T mutant alpha i-2 subunit of GTP-binding protein expressed in baculovirus-infected Sf9 cells. *J Biochem* 118:650–657.
- Itoh K, Brott BK, Bae GU, Ratcliffe MJ, Sokol SY. 2005. Nuclear localization is required for Dishevelled function in Wnt/beta-catenin signaling. *J Biol* 4:3.
- Izumi Y, Ohta N, Itoh-Furuya A, Fuse N, Matsuzaki F. 2004. Differential functions of G protein and Baz-aPKC signaling pathways in *Drosophila* neuroblast asymmetric division. *J Cell Biol* 164:729–738.
- Jameson EE, Roof RA, Whorton MR, Mosberg HI, Sunahara RK, Neubig RR, Kennedy RT. 2005. Real-time detection of basal and stimulated G protein GTPase activity using fluorescent GTP analogues. *J Biol Chem* 280:7712–7719.
- Johnston LA, Gallant P. 2002. Control of growth and organ size in *Drosophila*. *Bioessays* 24:54–64.
- Jung H, Kim HJ, Lee SK, Kim R, Kopachik W, Han JK, Jho EH. 2009. Negative feedback regulation of Wnt signaling by Gbg-mediated reduction of Dishevelled. *Exp Mol Med* [epub ahead of print].
- Katanaev VL, Buestorf S. 2009. Frizzled proteins are bona fide G protein-coupled receptors. Available from Nature Proceedings <http://hdl.handle.net/10101/npre.2009.2765.1>.
- Katanaev VL, Tomlinson A. 2006. Dual roles for the trimeric G protein Go in asymmetric cell division in *Drosophila*. *Proc Natl Acad Sci USA* 103:6524–6529.
- Katanaev VL, Ponzelli R, Semeriva M, Tomlinson A. 2005. Trimeric G protein-dependent frizzled signaling in *Drosophila*. *Cell* 120:111–122.
- Katanaev VL, Solis GP, Hausmann G, Buestorf S, Katanayeva N, Schrock Y, Stuermer CA, Basler K. 2008. Reggie-1/flotillin-2 promotes secretion of the long-range signalling forms of Wingless and Hedgehog in *Drosophila*. *Embo J* 27:509–521.
- Kimelman D, Xu W. 2006. beta-catenin destruction complex: insights and questions from a structural perspective. *Oncogene* 25:7482–7491.
- Kishida S, Yamamoto H, Ikeda S, Kishida M, Sakamoto I, Koyama S, Kikuchi A. 1998. Axin, a negative regulator of the wnt signaling pathway, directly interacts with adenomatous polyposis coli and regulates the stabilization of beta-catenin. *J Biol Chem* 273:10823–10826.
- Kopein D, Katanaev VL. 2009. *Drosophila* GoLoco-protein pins is a target of G $\alpha$ (o)-mediated G protein-coupled receptor signaling. *Mol Biol Cell* [epub ahead of print].
- Lecuit T, Brook WJ, Ng M, Calleja M, Sun H, Cohen SM. 1996. Two distinct mechanisms for long-range patterning by Decapentaplegic in the *Drosophila* wing. *Nature* 381:387–393.
- Li TR, White KP. 2003. Tissue-specific gene expression and ecdysone-regulated genomic networks in *Drosophila*. *Dev Cell* 5:59–72.
- Liu T, Liu X, Wang H, Moon RT, Malbon CC. 1999. Activation of rat frizzled-1 promotes Wnt signaling and differentiation of mouse F9 teratocarcinoma cells via pathways that require G $\alpha$ (q) and G $\alpha$ (o) function. *J Biol Chem* 274:33539–33544.
- Liu T, DeCostanzo AJ, Liu X, Wang H, Hallagan S, Moon RT, Malbon CC. 2001. G protein signaling from activated rat frizzled-1 to the beta-catenin-Lef-Tcf pathway. *Science* 292:1718–1722.
- Liu X, Rubin JS, Kimmel AR. 2005. Rapid, Wnt-induced changes in GSK3beta associations that regulate beta-catenin stabilization are mediated by G $\alpha$  proteins. *Curr Biol* 15:1989–1997.
- Logan CY, Nusse R. 2004. The Wnt signaling pathway in development and disease. *Annu Rev Cell Dev Biol* 20:781–810.
- Luo W, Lin SC. 2004. Axin: a master scaffold for multiple signaling pathways. *Neurosignals* 13:99–113.
- Malbon CC. 2005. G proteins in development. *Nat Rev Mol Cell Biol* 6:689–701.
- Malbon CC, Wang HY. 2006. Dishevelled: a mobile scaffold catalyzing development. *Curr Top Dev Biol* 72:153–166.
- Mao J, Wang J, Liu B, Pan W, Farr GH, 3rd, Flynn C, Yuan H, Takada S, Kimelman D, Li L, Wu D. 2001. Low-density lipoprotein receptor-related protein-5 binds to Axin and regulates the canonical Wnt signaling pathway. *Mol Cell* 7:801–809.
- McEwen DP, Gee KR, Kang HC, Neubig RR. 2001. Fluorescent BODIPY-GTP analogs: real-time measurement of nucleotide binding to G proteins. *Anal Biochem* 291:109–117.
- Milligan G, Kostenis E. 2006. Heterotrimeric G-proteins: a short history. *Br J Pharmacol* 147(Suppl 1):S46–55.
- Nakamura T, Hamada F, Ishidate T, Anai K, Kawahara K, Toyoshima K, Akiyama T. 1998. Axin, an inhibitor of the Wnt signalling pathway, interacts with beta-catenin, GSK-3beta and APC and reduces the beta-catenin level. *Genes Cells* 3:395–403.
- Neumann CJ, Cohen SM. 1996. A hierarchy of cross-regulation involving Notch, wingless, vestigial and cut organizes the dorsal/ventral axis of the *Drosophila* wing. *Development* 122:3477–3485.
- Nolo R, Abbott LA, Bellen HJ. 2000. Senseless, a Zn finger transcription factor, is necessary and sufficient for sensory organ development in *Drosophila*. *Cell* 102:349–362.
- Northup JK, Sternweis PC, Gilman AG. 1983. The subunits of the stimulatory regulatory component of adenylate cyclase. Resolution, activity, and properties of the 35,000-dalton (beta) subunit. *J Biol Chem* 258:11361–11368.
- Polakis P. 2007. The many ways of Wnt in cancer. *Curr Opin Genet Dev* 17:45–51.
- Punehiwea C, Ferreira AM, Cassell R, Rodrigues P, Fujii N. 2009. Sequence requirement and subtype specificity in the high-affinity interaction between human frizzled and dishevelled proteins. *Protein Sci* 18:994–1002.
- Reya T, Clevers H. 2005. Wnt signalling in stem cells and cancer. *Nature* 434:843–850.
- Schwarz-Romond T, Metcalfe C, Bienz M. 2007. Dynamic recruitment of axin by Dishevelled protein assemblies. *J Cell Sci* 120:2402–2412.
- Shimada Y, Usui T, Yanagawa S, Takeichi M, Uemura T. 2001. Asymmetric colocalization of Flamingo, a seven-pass transmembrane cadherin, and Dishevelled in planar cell polarization. *Curr Biol* 11:859–863.



- Siderovski DP, Strockbine B, Behe CI. 1999. Whither goest the RGS proteins? *Crit Rev Biochem Mol Biol* 34:215–251.
- Simons M, Gault WJ, Gotthardt D, Rohatgi R, Klein TJ, Shao Y, Lee HJ, Wu AL, Fang Y, Satlin LM, Dow JT, Chen J, Zheng J, Boutros M, Mlodzik M. 2009. Electrochemical cues regulate assembly of the Frizzled/Dishevelled complex at the plasma membrane during planar epithelial polarization. *Nat Cell Biol* 11:286–294.
- Stemmler LN, Fields TA, Casey PJ. 2006. The regulator of G protein signaling domain of axin selectively interacts with G $\alpha$ 12 but not G $\alpha$ 13. *Mol Pharmacol* 70:1461–1468.
- Sternweis PC, Robishaw JD. 1984. Isolation of two proteins with high affinity for guanine nucleotides from membranes of bovine brain. *J Biol Chem* 259:13806–13813.
- Takacs CM, Baird JR, Hughes EG, Kent SS, Benchabane H, Paik R, Ahmed Y. 2008. Dual positive and negative regulation of wingless signaling by adenomatous polyposis coli. *Science* 319:333–336.
- Takei Y, Ozawa Y, Sato M, Watanabe A, Tabata T. 2004. Three *Drosophila* EXT genes shape morphogen gradients through synthesis of heparan sulfate proteoglycans. *Development* 131:73–82.
- Tamai K, Zeng X, Liu C, Zhang X, Harada Y, Chang Z, He X. 2004. A mechanism for Wnt coreceptor activation. *Mol Cell* 13:149–156.
- Tanimoto H, Itoh S, ten Dijke P, Tabata T. 2000. Hedgehog creates a gradient of DPP activity in *Drosophila* wing imaginal discs. *Mol Cell* 5:59–71.
- Tolwinski NS, Wieschaus E. 2004. Rethinking WNT signaling. *Trends Genet* 20:177–181.
- Tolwinski NS, Wehrli M, Rives A, Erdeniz N, DiNardo S, Wieschaus E. 2003. Wg/Wnt signal can be transmitted through arrow/LRP5,6 and Axin independently of Zw3/Gsk3 $\beta$  activity. *Dev Cell* 4:407–418.
- Wang HY, Liu T, Malbon CC. 2006. Structure-function analysis of Frizzleds. *Cell Signal* 18:934–941.
- Wedegaertner PB, Wilson PT, Bourne HR. 1995. Lipid modifications of trimeric G proteins. *J Biol Chem* 270:503–506.
- Willert K, Jones KA. 2006. Wnt signaling: is the party in the nucleus? *Genes Dev* 20:1394–1404.
- Willert K, Logan CY, Arora A, Fish M, Nusse R. 1999. A *Drosophila* Axin homolog, Daxin, inhibits Wnt signaling. *Development* 126:4165–4173.
- Wong HC, Bourdelas A, Krauss A, Lee HJ, Shao Y, Wu D, Mlodzik M, Shi DL, Zheng J. 2003. Direct binding of the PDZ domain of Dishevelled to a conserved internal sequence in the C-terminal region of Frizzled. *Mol Cell* 12:1251–1260.
- Yanagawa S, van Leeuwen F, Wodarz A, Klingensmith J, Nusse R. 1995. The dishevelled protein is modified by wingless signaling in *Drosophila*. *Genes Dev* 9:1087–1097.
- Yokoyama N, Yin D, Malbon CC. 2007. Abundance, complexation, and trafficking of Wnt/beta-catenin signaling elements in response to Wnt3a. *J Mol Signal* 2:11.
- Zeng L, Fagotto F, Zhang T, Hsu W, Vasicek TJ, Perry WL, 3rd, Lee JJ, Tilghman SM, Gumbiner BM, Costantini F. 1997. The mouse Fused locus encodes Axin, an inhibitor of the Wnt signaling pathway that regulates embryonic axis formation. *Cell* 90:181–192.
- Zeng X, Tamai K, Doble B, Li S, Huang H, Habas R, Okamura H, Woodgett J, He X. 2005. A dual-kinase mechanism for Wnt co-receptor phosphorylation and activation. *Nature* 438:873–877.